

THE FIRST BROWN DWARF/PLANETARY-MASS OBJECT IN THE 32 ORIONIS GROUP

ADAM J. BURGASSER¹, MIKE A. LOPEZ¹, ERIC E. MAMAJEK², JONATHAN GAGNÉ³, JACQUELINE K. FAHERTY^{4,5,6}, MELISA TALLIS¹, CALEB CHOBAN¹, IVANNA ESCALA¹ AND CHRISTIAN AGANZE^{1,7}

Accepted to *ApJ* 2016 Feb 8

ABSTRACT

The 32 Orionis group is a co-moving group of roughly 20 young (24 Myr) M3-B5 stars 100 pc from the Sun. Here we report the discovery of its first substellar member, WISE J052857.69+090104.2. This source was previously reported to be an M giant star based on its unusual near-infrared spectrum and lack of measureable proper motion. We re-analyze previous data and new moderate-resolution spectroscopy from Magellan/FIRE to demonstrate that this source is a young near-infrared L1 brown dwarf with very low surface gravity features. Spectral model fits indicate $T_{\text{eff}} = 1880_{-70}^{+150}$ K and $\log g = 3.8_{-0.2}^{+0.2}$, consistent with a 15–22 Myr object with a mass near the deuterium-burning limit. Its sky position, estimated distance, kinematics (both proper motion and radial velocity), and spectral characteristics are all consistent with membership in 32 Orionis, and its temperature and age imply a mass ($M = 14_{-3}^{+4} M_J$) that straddles the brown dwarf/planetary-mass object boundary. The source has a somewhat red $J - W2$ color compared to other L1 dwarfs, but this is likely a low-gravity-related temperature offset; we find no evidence of significant excess reddening from a disk or cool companion in the 3–5 μm waveband.

Keywords: open clusters and associations: individual (32 Orionis) — stars: individual (WISE J052857.69+090104.2) — stars: late-type — stars: low mass, brown dwarfs — stars: pre-main sequence

1. INTRODUCTION

Current star formation theory holds that the vast majority of stars form in clusters or groups, although whether most come from massive star-forming regions or low-density associations remains a matter of ongoing debate (Adams & Myers 2001; Lada & Lada 2003; Bressert et al. 2010; Koenig & Leisawitz 2014). The origin of brown dwarfs, objects with insufficient mass to fuse hydrogen ($M \lesssim 0.07 M_{\odot}$; Kumar 1962, 1963; Hayashi & Nakano 1963) is even more uncertain, as these sources are detectable only at relatively short distances, roughly out to the Orion Nebula Cluster (ONC) and Ori OB1 subgroups ($d \approx 400$ pc). Young brown dwarfs are increasingly being found in nearby ($d \lesssim 100$ pc) sparse associations and moving groups (Zuckerman & Song 2004; López-Santiago et al. 2006; Torres et al. 2008; Gizis 2002; Schlieder et al. 2010; Gagné et al. 2014, 2015b) thanks to the infrared sensitivity and multi-epoch astrometry provided by the 2 Micron All Sky Survey (2MASS; Skrutskie et al. 2006) and the Wide-field Infrared Survey Explorer (WISE;

Wright et al. 2010), among others. The organizations of these groupings vary considerably, and include clusters, or coeval groups of gravitational bound stars; associations, or coeval groups of stars that are gravitationally unbound and will disperse over $\approx 10^7$ – 10^8 yr; and moving groups or streams, which also have common kinematics but may or may not be coeval (Zuckerman & Song 2004; López-Santiago et al. 2006; Torres et al. 2008). Unlike massive star clusters, nearby associations and moving groups are more widely dispersed and have fewer stars ($\lesssim 10^2$ vs 10^4 for the ONC), making the detection of members challenging. As such, the populations of the most common nearby associations remain incomplete, particularly at substellar masses. Identification and study of brown dwarfs in these systems is essential for characterizing the birth sites and formation processes for the Galactic brown dwarf population, as well as characterizing the influence of age and mass on atmospheric chemistry (e.g., cloud-formation; Burgasser et al. 2008;Looper et al. 2008; Barman et al. 2011), investigating disk and planet formation and evolution as a function of primary mass (e.g., Jayawardhana et al. 2002; Luhman et al. 2005), and identifying analogs of young exoplanetary systems (e.g., Marois et al. 2008; Lafrenière et al. 2010; Delorme et al. 2013; Faherty et al. 2013; Gauza et al. 2015).

Recently, Thompson et al. (2013) reported the detection of a faint infrared source WISE J052857.68+090104.4 (hereafter WISE J0528+0901) whose near-infrared spectrum exhibits features consistent with very low surface gravity. Due to the lack of measureable proper motion in the original WISE data, they concluded that this source is an M giant star. In this paper, we demonstrate that this source is a young L-type brown dwarf/planetary

¹ Department of Physics, University of California, San Diego, CA 92093, USA; aburgasser@ucsd.edu

² Department of Physics and Astronomy, University of Rochester, Rochester, NY 14627-0171, USA

³ Institut de Recherche sur les Exoplanètes (iREx), Université de Montréal, Département de Physique, C.P. 6128 Succ. Centre-ville, Montréal, QC H3C 3J7, Canada

⁴ Department of Terrestrial Magnetism, Carnegie Institution of Washington, Washington, DC 20015, USA

⁵ Department of Astrophysics, American Museum of Natural History, Central Park West at 79th Street, New York, NY 10024, USA

⁶ Hubble Fellow

⁷ Department of Physics and Dual-Degree Engineering, Morehouse College, 830 Westview Drive S.W., Atlanta, GA 30314, USA

mass object and the first substellar member of the 24 Myr-old 32 Orionis group (Mamajek 2007; Shvonski et al. 2010; Bell et al. 2015). In Section 2 we present new near-infrared spectroscopic measurements of WISE J0528+0901 obtained with the Folded-port InfraRed Echellette spectrograph (FIRE; Simcoe et al. 2013) at the Magellan Telescopes. In Section 3 we re-analyze the Thompson et al. spectrum by comparing to equivalent data of field and young brown dwarfs in the SpeX Prism Library (SPL, Burgasser 2014). This analysis demonstrates that WISE J0528+0901 is a near-clone to a previously-identified young brown dwarf in the 23 Myr-old β Pictoris Moving Group, and we derive temperature and gravity classifications that support its low temperature and surface gravity. In Section 4 we compare the near-infrared spectrum to atmosphere models to determine the physical properties of WISE J0528+0901 and confirm its youth. In Section 5 we examine spatial and kinematic evidence of membership in 32 Orionis. Our results are discussed in Section 6.

2. FIRE OBSERVATIONS

We obtained new moderate-resolution near-infrared spectral data of WISE J0528+0901 with Magellan/FIRE on 2013 December 12 (UT), in clear conditions and 0".8 seeing at J -band. We used the cross-dispersed echellette mode and 0".6 slit to obtain 0.8–2.45 μm spectroscopy at a resolving power $\lambda/\Delta\lambda \approx 6000$. Four exposures of 900 s each were obtained at different positions along the slit and at an airmass of 1.29. This was followed by observations of the A0 V star HD 33831 ($V = 8.02$) for telluric correction, flux calibration, and first-order correction of wavelength-dependent slit losses; and ThAr emission lamps for wavelength calibration. We obtained high- and low-illumination flat fields at the beginning of the night for pixel response calibration. All data were reduced using an updated version of the Interactive Data Language (IDL) pipeline FIREHOSE (Gagné et al. 2015a), which is based on the MASE (Bochanski et al. 2009) and SpeXTool (Vacca et al. 2003; Cushing et al. 2004) packages.

The reduced spectrum is shown in Figure 1, compared to the SpeX spectrum of Thompson et al. (2013) which was used to guide our relative scaling of the individual FIRE orders. The FIRE spectrum appears comparatively noisier, but much of the structure seen arises from overlapping molecular transitions of H_2O , FeH, CO and VO present in the atmosphere of WISE J0528+0901. The data sufficiently resolve the K I doublets at 1.17 μm ($3p^64p \rightarrow 3p^63d$) and 1.25 μm ($3p^64p \rightarrow 3p^65s$), which we find to be much weaker in strength than those of field late-M and L dwarfs (equivalent widths = $3.0 \pm 0.2 \text{ \AA}$ versus 5–10 \AA for M9–L1 dwarfs; McLean et al. 2003). We used the three lines at⁸ 1.1693442 μm , 1.2435700 μm and 1.2525591 μm to measure a heliocentric radial velocity (RV) for WISE J0528+0901 of $+18 \pm 3 \text{ km s}^{-1}$, where the uncertainty includes both scatter in the line measurements and 0.8 km s^{-1} uncertainty in the wavelength calibration.

⁸ Line centers are in vacuum wavelengths and are from the NIST Atomic Line Spectral Database (Ralchenko et al. 2011).

3. RE-ANALYSIS OF SPEX DATA

We re-examined the classification of WISE J0528+0901 by Thompson et al. (2013) by comparing its SpeX spectrum to the M and L dwarf spectral standards defined in Kirkpatrick et al. (2010). Following the prescription of that study, we compared the target spectrum ($T[\lambda]$) to standard spectra ($S_k[\lambda]$ for spectral type k) over the 0.9–1.4 μm wavelength range using a χ^2 statistic,

$$\chi_k^2 = \sum_{\lambda_i=0.9 \mu\text{m}}^{1.4 \mu\text{m}} \frac{(T[\lambda_i] - \alpha S_k[\lambda_i])^2}{\sigma_T[\lambda_i]^2}, \quad (1)$$

where the denominator includes only the uncertainty of the WISE J0528+0901 spectrum. The optimized scale factor is

$$\alpha_k = \left[\sum_{\lambda_i=0.9 \mu\text{m}}^{1.4 \mu\text{m}} \frac{S_k[\lambda_i]T[\lambda_i]}{\sigma_T[\lambda_i]^2} \right] / \left[\sum_{\lambda_i=0.9 \mu\text{m}}^{1.4 \mu\text{m}} \frac{S_k[\lambda_i]^2}{\sigma_T[\lambda_i]^2} \right] \quad (2)$$

(cf. Cushing et al. 2008). The best match was to the L1 standard 2MASSW J2130446–084520 (Kirkpatrick et al. 2008; Figure 2). However, as originally noted by Thompson et al. (2013), there are several distinct peculiarities in the spectrum of WISE J0528+0901, including an unusually peaked H -band (1.7 μm) continuum; weak FeH (1.0 μm), CO (2.3 μm) and Na I (2.2 μm) absorption features; and a prominent 1.05 μm VO band. All of these features are indicators of low surface gravity (Lucas et al. 2001; Gorlova et al. 2003; Allers et al. 2007; Allers & Liu 2013). We computed additional classifications using the spectral index-based methods of Reid et al. (2001) and Allers & Liu (2013), which yielded types of $L1.8 \pm 0.8$ and $L0.5 \pm 0.5$, respectively.⁹ The near-infrared spectrum of WISE J0528+0901 appears to be that of a peculiar and possibly young L1 dwarf.

We then compared the SpeX spectrum to all 911 optically-classified M5–L5 dwarfs in the SPL. In this case, spectra were compared using the same χ^2 statistic but over the ranges 0.80–1.35 μm , 1.42–1.80 μm and 1.92–2.45 μm to avoid regions of strong telluric absorption. The best-matching spectrum (Figure 2) is that of 2MASS J06085283–2753583 (hereafter 2MASS J0608–2753), a brown dwarf member of the 23 ± 3 Myr β Pictoris Moving Group¹⁰ (Rice et al. 2010; Mamajek & Bell 2014). The spectrum of 2MASS J0608–2753 exhibits the same peculiarities as that of WISE J0528+0901, but with slightly weaker VO and H_2O features and a bluer overall spectrum.

Kirkpatrick et al. (2008) reported an optical classification of M8.5 γ for 2MASS J0608–2753, the suffix indicating very low surface gravity features in the red

⁹ Uncertainties include propagation of spectrum measurement uncertainties and systematic uncertainty in relations.

¹⁰ Gagné et al. (2014) argued that 2MASS J0608–2753 is a candidate member of the 42_{-4}^{+6} Myr Columba association (Zuckerman et al. 2011; Bell et al. 2015), although the XYZ Galactic coordinates and UVW space velocities are somewhat discrepant. Re-examination of these quantities using the original proper motion in Rice et al. (2010) make β Pictoris a better kinematic match than Columba.

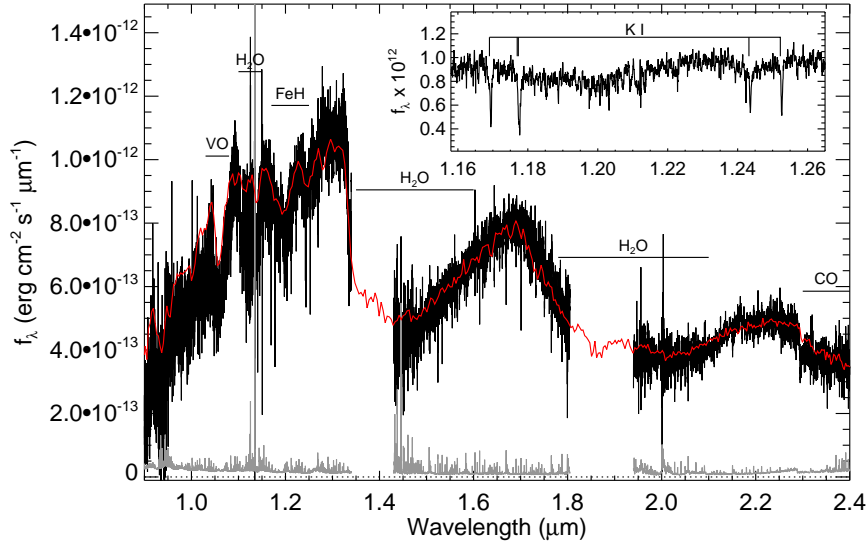


Figure 1. Magellan/FIRE spectrum of WISE J0528+0901 (black line) compared to IRTF/SpeX data from Thompson et al. (2013, red line). Both spectra are scaled to the apparent 2MASS K_s magnitude of the source. The uncertainty spectrum for the FIRE data is shown in grey. Primary molecular absorption features are labeled, while regions of strong telluric absorption have been masked. The inset box displays the 1.160–1.265 μm region to highlight the K I lines present in the FIRE spectrum used for RV measurement.

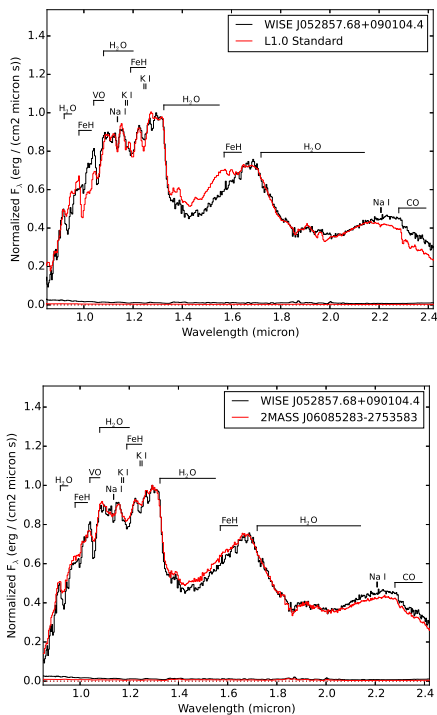


Figure 2. IRTF/SpeX near-infrared spectrum of WISE J0528+0901 (black line) compared to data for the L1 spectral standard 2MASSW J2130446–084520 (top panel, red line; data from Bardalez Gagliuffi et al. 2014) and the young brown dwarf 2MASS J0608–2753 (bottom panel, red line; data from Allers & Liu 2013). The spectrum of WISE J0528+0901 is normalized at 1.27 μm ; the comparison spectra are normalized to their optimal scaling factors (see Eqn 2). Uncertainty spectra are indicated at bottom. Key absorption features are labeled.

optical region (see also Cruz et al. 2009). We determined equivalent near-infrared gravity classifications for WISE J0528+0901 and 2MASS J0608–2753 using the index-based scheme of Allers & Liu (2013), which com-

pares the gravity-sensitive features of FeH, VO, K I and H -band continuum shape. Both spectra had gravity scores of VLG (very low gravity), consistent with prior analysis of 2MASS J0608–2753 by Allers & Liu (2013); Gagné et al. (2015b). Other VLG-classified brown dwarfs reported in that and subsequent studies (e.g., Artigau et al. 2015; Gagné et al. 2015b) are members of young associations with ages of 5–30 Myr. Allers & Liu (2013) and Gagné et al. (2015b) also classified 2MASS J0608–2753 as an L0 dwarf in the near-infrared, consistent with our classifications based on comparison to standards ($L0.5 \pm 0.5$) and indices ($L0.9 \pm 0.8$ for Reid et al. 2001). It has been previously noted that young brown dwarfs have optical classifications that are up to 3 types earlier than their near-infrared types (Kirkpatrick et al. 2008).

4. ATMOSPHERIC MODEL FITTING

To more quantitatively characterize the physical properties of WISE J0528+0901, we compared the Thompson et al. spectrum to solar-metallicity BT-Settl atmosphere models (Allard et al. 2012) over an effective temperature (T_{eff}) range of 400–2900 K and a log surface gravity ($\log g$) range of 3.5–5.5 (units of cm s^{-2}). Models were smoothed to the equivalent resolution of the data using a Hamming filter (Blackman & Tukey 1958), and interpolated from the initial grid (steps of 100 K in T_{eff} and 0.5 dex in $\log g$) by linearly interpolating the logarithm of fluxes. We compared the observed spectrum to the models, avoiding the telluric bands, using the same χ^2 statistic as above, and explored parameter space using a custom Markov Chain Monte Carlo (MCMC) code with a Metropolis-Hastings algorithm (Metropolis et al. 1953; Hastings 1970). We started with an initial $T_{\text{eff}} = 2100$ K, based on its L1 near-infrared classification and the T_{eff} /spectral-type relations of Stephens et al. (2009), Marocco et al. (2013), and Filippazzo et al. (2015); and an initial $\log g = 4.5$ based on its low surface gravity classification. We then computed a chain of 10^5 steps,

alternately updating $\vec{\theta} = (T_{\text{eff}}, \log g)$ by random draws from a normal distribution, at each i^{th} parameter step:

$$P(\theta_{(i+1)}|\theta_{(i)}) \propto e^{-\frac{(\theta_{(i+1)} - \theta_{(i)})^2}{2\sigma_{\theta}^2}} \quad (3)$$

where $\sigma_{T_{\text{eff}}} = 50$ K and $\sigma_{\log g} = 0.25$ dex. The criterion to adopt successive parameters was based on the F-test cumulative distribution function (FCDF),

$$U(0,1) < 1 - \text{FCDF} \left(\frac{\chi_{(i+1)}^2}{\chi_{(i)}^2}, \text{DOF}, \text{DOF} \right) \quad (4)$$

where $U(0,1)$ is a random number drawn from a uniform distribution between 0 and 1 and $\text{DOF} = 169$ is the number of degrees of freedom in the fit, accounting for the resolution of the spectral data and two model parameters¹¹. We eliminated the first 10% of the chain and then evaluated the distributions of T_{eff} and $\log g$ parameters for the remainder.

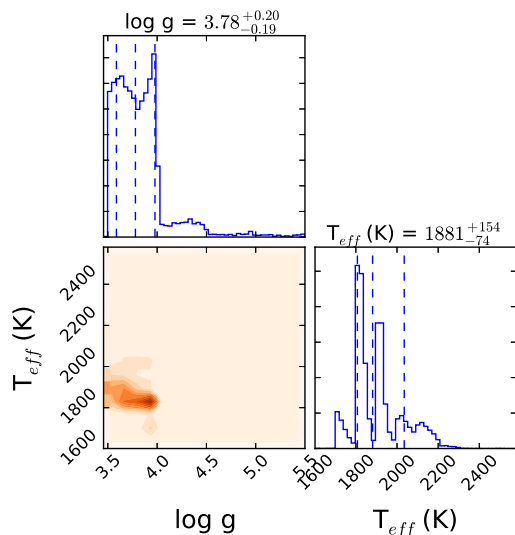


Figure 3. T_{eff} and $\log g$ parameter distributions from our MCMC analysis comparing BT-Settl models to the SpeX data for WISE J0528+0901. The lower left corner shows the probability density distribution of our two parameters, determined as a percentage of all MCMC chain steps, with color contours ranging from 0% (light) to 90% (dark) in steps of 20%. This distribution indicates a slight negative correlation between the parameters, with higher T_{eff} s matching to lower surface gravities. Marginalized one-dimensional parameter distributions are shown on the wings, with median and 16% and 84% quantiles labeled and listed. Note that structure in the T_{eff} distribution arises from our model interpolation scheme. This plot was generated using code by Foreman-Mackey et al. (2014).

Table 1 lists the best-fit and median parameter values, while Figure 3 displays the distributions of and correlation between T_{eff} and $\log g$. The surface gravity distribution abuts the lower limit of our models, but is constrained to $\log g \lesssim 4.0$, while T_{eff} is constrained to 1800–2000 K; i.e., about 200 K cooler than the T_{eff} estimate

¹¹ We had previously employed a pure exponential, $U(0,1) < e^{-0.5(\chi_{(i+1)}^2 - \chi_{(i)}^2)}$, as a step criterion (e.g., Aganze et al. 2015), but found this to be overly discriminatory due to the large values of χ^2 involved. The FCDF properly accounts for the degrees of freedom in the fit.

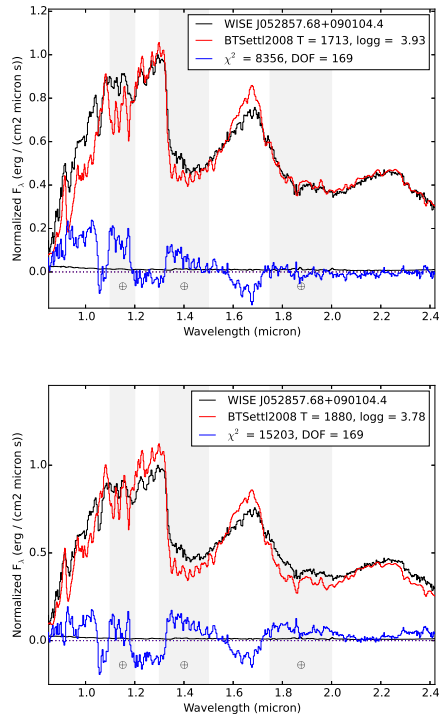


Figure 4. SpeX near-infrared spectrum of WISE J0528+0901 (black line) compared to the best-fit BT-Settl model from MCMC analysis (top panel) and the model corresponding to the median parameters (bottom panel). The spectrum of WISE J0528+0901 is normalized at $1.27 \mu\text{m}$, while the spectra of the atmosphere models (red lines) are normalized to their optimized scaling factors (Eqn. 2). The difference spectra (WISE J0528+0901 - Model) are shown as blue lines. The resulting χ^2 values and degrees of freedom (DOF) are listed in the inset boxes. Regions of strong telluric absorption not included in the fit are indicated by vertical gray bands.

based on its spectral type. Both distributions exhibit structure due to the model interpolation scheme. We find median parameters of $T_{\text{eff}} = 1880^{+150}_{-70}$ K and $\log g = 3.8^{+0.2}_{-0.2}$, where the uncertainties correspond to the 16% and 84% quantiles of the marginalized parameter distributions. The best-fit model is shown in Figure 4, and has $T_{\text{eff}} = 1713$ K and $\log g = 3.93$. This model reasonably represents the overall spectral energy distribution of WISE J0528+0901, but shows large deviations around the $1.05 \mu\text{m}$ VO band, overly strong H_2O at $0.9 \mu\text{m}$ and $1.4 \mu\text{m}$, and too sharp of an H -band peak. With $\chi^2 = 8356$ for 169 degrees of freedom, this model is clearly not a precise representation of the data. The best-fit temperature is also a significant outlier as compared to the inferred T_{eff} distribution. The disagreements between spectral models and data necessitate some skepticism in the parameters inferred from the best-fit model.

We attempted to infer physical parameters (mass and age) from our model-fit parameters and the evolutionary models of Baraffe et al. (2003). This proved to be challenging as the model parameters span an epoch (10–50 Myr) of active deuterium fusion in low-mass brown dwarfs (15–30 M_J), sparsely sampled in the evolutionary models, during which the thermal pressure briefly reverses the general trend of decreasing surface gravity with decreasing mass via radius expansion (Burrows et al. 2001; Baraffe et al. 2003; Spiegel et al.

Table 1
Results from MCMC Model Fitting Analysis

Parameter	Best-Fit	Median Value ^a
T_{eff} (K)	1713	1880^{+150}_{-70}
$\log g$ (K)	3.93	$3.8^{+0.2}_{-0.2}$
Age (Myr) ^a	21	18^{+4}_{-17}
Mass (M_J) ^a	13	13^{+3}_{-6}
Radius (R_{\odot}) ^a	0.15	$0.18^{+0.03}_{-0.02}$
χ^2 (DOF)	8356 (169)	...

^a Based on the T_{eff} and $\log g$ parameter distributions and evolutionary models of Baraffe et al. (2003).

2011). Interpolation over this feature produces large uncertainties in the inferred age ($\tau = 18^{+4}_{-17}$ Myr) and mass¹² ($M = 13^{+3}_{-6} M_J$) of WISE J0528+0901. Nevertheless, the age is similar to that of β Pictoris and, as discussed below, 32 Orionis, while the mass straddles the deuterium-burning boundary. We re-examine the physical properties of WISE J0528+0901 in Section 6.

5. ASSOCIATION OF WISE J0528+0901 WITH 32 ORIONIS

WISE J0528+0901 is spatially aligned with several young associations and star forming regions in the general direction of Orion, although it is too nearby to be a member of the any of the Orion OB1 subgroups; e.g., λ Orionis or Ori OB1a (Genzel & Stutzki 1989). Comparing its apparent 2MASS magnitudes to the absolute magnitude scale of Dupuy & Liu (2012) for spectral types of M9 and L1 (which encompass both its near-infrared and likely optical classifications; see Section 3), we find mean distances of 96 ± 11 pc to 74 ± 8 pc, respectively, or a combined average of 81 ± 13 pc (Table 2). We also computed the corresponding distances for the WISE $W2$ band and found these to be 30% smaller, suggesting excess flux at $5 \mu\text{m}$. Indeed, the $J - W2 = 2.62 \pm 0.12$ color for WISE J0528+0901 is unusually red for M9–L1 dwarfs, even among young sources (Faherty et al. 2012; Filippazzo et al. 2015). This feature is discussed further in the following section. Note that these distances are likely underestimated, as the Dupuy & Liu (2012) relation is defined for evolved field dwarfs. Young late-M and L dwarfs (10–100 Myr) are generally found to be overluminous in these bands, due to their larger radii and spectral classification offsets (Dupuy & Liu 2012; Faherty et al. 2012; Filippazzo et al. 2015).

Within the uncertainties, WISE J0528+0901 is roughly at the distance of the B5+B7 star 32 Orionis (93^{+6}_5 pc, van Leeuwen 2007), separated by only 3:1 on the sky. Mamajek (2007) first identified a co-moving group of X-ray-bright T Tauri stars around 32 Orionis; and Bell et al. (2015) have analyzed the kinematics, disc fraction and age diagnostics of 20 co-moving members, determining an isochronal age of 24^{+4}_{-3} Myr. Kharchenko et al. (2013) have also identified this system, characterizing it as an open cluster with an isochronal age of 32 Myr. The system exhibits modest reddening, E(B-

V) = 0.04 ± 0.02 . Figure 5 compares the equatorial sky coordinates of 32 Orionis members¹³ to those of WISE J0528+0901. While slightly outside the “core” of the group, WISE J0528+0901 is still within the 2σ dispersion ellipse of members on the sky. We also compared the Galactic XYZ positions of the five 32 Orionis members with HIPPARCOS parallaxes (32 Orionis, HD 34500, HD 35656, HD 35714 and HD 36823; van Leeuwen 2007) to that of WISE J0528+0901, assuming its M9 dwarf distance. WISE J0528+0901 is spatially coincident with the member stars, overlapping a 3σ dispersion sphere in all three dimensions. There is therefore strong spatial evidence that WISE J0528+0901 is a member of 32 Orionis.

With regard to kinematics, Mamajek (2007) report a mean $\vec{\mu} = (+7, -33)$ mas yr⁻¹ for group members. We performed a new cross-match of 2MASS¹⁴ and WISE sources in the vicinity of WISE J0528+0901 and found $\vec{\mu} = (-11 \pm 10, -39 \pm 12)$ mas yr⁻¹ for this source, inconsistent with the zero motion reported by Thompson et al. (2013) but consistent with the mean motion of group members. 32 Orionis itself has a heliocentric RV of $+18.6 \pm 1.2$ km s⁻¹ (Kharchenko et al. 2007), which is identical to the RV measured here for WISE J0528+0901.

6. DISCUSSION

The observed and estimated physical properties of WISE J0528+0901 are summarized in Table 3. Spectral, spatial and kinematic evidence are mutually consistent with WISE J0528+0901 being a young substellar object and member of the 32 Orionis group. The isochronal age of this system, 24^{+4}_{-3} Myr (Bell et al. 2015), is similar to the age inferred from spectral and evolutionary model analysis, as well as that of WISE J0528+0901’s β Pictoris counterpart, 2MASS J0608–2753. At this age, the estimated mass from the Baraffe et al. (2003) evolutionary models, assuming a conservative estimate of $T_{\text{eff}} = 1900 \pm 250$ K (which encompasses the temperature range inferred from our model fits), is $14^{+4}_{-3} M_J$, again overlapping the deuterium-burning limit. The estimated $\log g$ from the evolutionary models is $4.16^{+0.04}_{-0.08}$, only 1.3σ higher than the atmospheric model fits. We also examined predictions from the Saumon & Marley (2008) evolutionary models which include cloud opacity effects in brown dwarf thermal evolution, and found identical values for mass ($M = 14^{+2}_{-2} M_J$) and surface gravity ($\log g = 4.12^{+0.05}_{-0.10}$), whether or not cloud opacity is included. There is therefore good agreement between spectral and evolutionary model analyses for this source, assuming it is a 32 Orionis group member.

The additional agreement in the spectral peculiarities between WISE J0528+0901 and its similarly-aged counterpart 2MASS J0608–2753 supports the conjec-

¹³ Bouy & Alves (2015) have recently proposed the bright star Bellatrix (γ Orionis) as a member of the 32 Orionis group based on its position and age; however, the proper motion of this source is sufficiently discrepant from the mean of the other members that its 3D velocity differs by 12 km s⁻¹, a 10σ discrepancy. We have chosen not to include this source in our comparative analysis until the membership of the naked eye star can be confirmed.

¹⁴ Thompson et al. (2013) did not make use of 2MASS astrometry for WISE J0528+0901 as it appears only in the 2MASS Reject Table (Cutri et al. 2003) due to a mis-labeled artifact flag in the J -band.

¹² $1 M_J = 1$ jovian mass = $0.000955 M_{\odot}$. Reported uncertainties on mass and age again reflect the 16% and 84% quantiles.

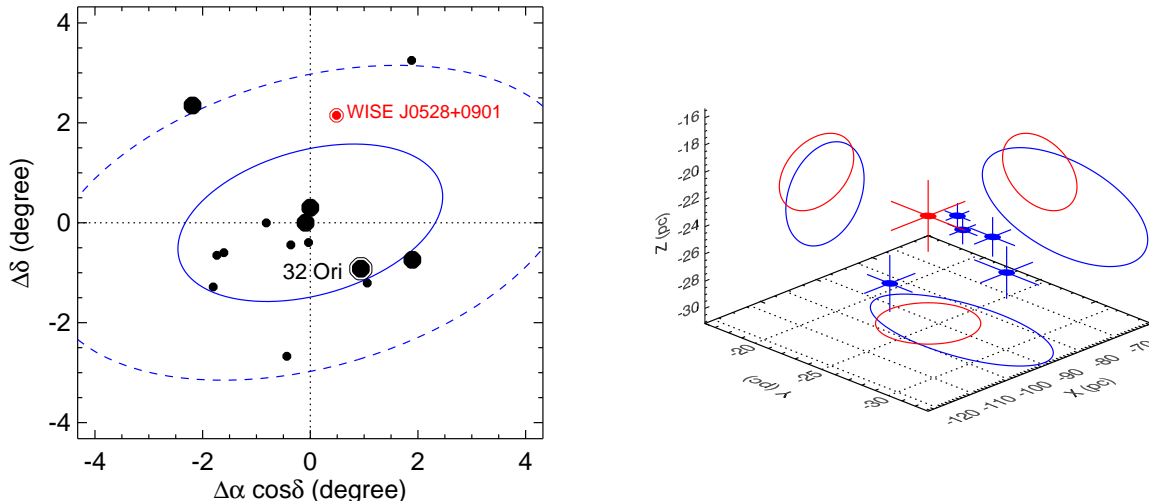


Figure 5. (Left) Sky positions of 32 Orionis members listed in Bell et al. (2015, black points) and WISE J0528+0901 (red point), relative to the mean sky position of the former. Large symbols indicate the five 32 Ori members with parallax measurements. 1σ (solid line) and 2σ (dashed line) dispersion ellipses for group members are indicated. (Right) Galactic XYZ coordinates of the 32 Orionis members with parallax measurements (blue points) compared to WISE J0528+0901, assuming a distance of 98 ± 11 pc; i.e., consistent with an M9 spectral type. The projected 3σ dispersion (blue lines) and error ellipse for WISE J0528+0901 (red line) are indicated. Note that the coordinate system shown is centered on the Sun.

Table 2
Distance Estimates for WISE J0528+0901^a

Filter	Apparent Mag	M9		L1	
		Absolute Mag	d (pc)	Absolute Mag	d (pc)
2MASS J	16.26 ± 0.12	11.3 ± 0.4	102 ± 21	12.0 ± 0.4	72 ± 12
2MASS H	15.44 ± 0.13	10.6 ± 0.4	93 ± 18	11.1 ± 0.4	77 ± 15
2MASS K_s	14.97 ± 0.12	10.1 ± 0.4	94 ± 18	10.7 ± 0.4	75 ± 15
WISE $W2$	13.64 ± 0.04	9.6 ± 0.4	65 ± 11	10.1 ± 0.4	52 ± 7
SpT Average ^b			96 ± 11		74 ± 8
Overall Average ^b			81 ± 13		
32 Orionis ^c			93 ± 5		

^a Based on the absolute magnitude/spectral type relations of Dupuy & Liu (2012).

^b Combining only 2MASS JHK_s distances.

^c Based on the HIPPARCOS parallaxes of five 32 Orionis members (van Leeuwen 2007).

ture that these features are consistent metrics of age. Nevertheless, WISE J0528+0901 itself appears to be unusually red in $J - W2$ color as compared to its young counterparts, in excess of cluster reddening. Condensate cloud effects may play an important role in these color differences (Allers & Liu 2013; Faherty et al. 2013; Gizis et al. 2015), but so can circumstellar structure: disks and planetary companions (Looper et al. 2010a,b; Schneider et al. 2012). On the other hand, Filippazzo et al. (2015) have shown that young L dwarfs can be up to 300 K cooler than equivalently (optically) classified field sources, and that this lower temperature provides an explanation for the red $J - W2$ colors. For WISE J0528+0901, we find evidence that this last explanation is the most likely. Our model-fit temperature is about ≈ 200 K cooler than other L1 field dwarfs, and our median-parameter spectral model is also a better match to the overall near-infrared spectral energy distribution (SED) of WISE J0528+0901 than a warmer model (Figure 6). The median-parameter SED ($\chi^2 = 11.1$ for

the 2MASS JHK_s and WISE $W1$ and $W2$ bands) requires no significant $3-5 \mu\text{m}$ excess, and the scale factor to align this model with the photometry corresponds to a radius of $0.18\pm 0.02 R_\odot$, which is consistent with predictions for the radius of a $T_{\text{eff}} = 1880$ K, 25 Myr-old brown dwarf from evolutionary models ($0.16 R_\odot$ for Baraffe et al. 2003). In contrast, a very low gravity L1 dwarf model ($T_{\text{eff}} = 2100$ K, $\log g = 4.0$) requires significant reddening to match the data, and a radius much smaller ($0.13\pm 0.02 R_\odot$) than predicted by evolutionary models ($0.17 R_\odot$). Given the consistency of our spectral and evolutionary modeling analyses for our median-fit parameters, we conclude that WISE J0528+0901 is cooler than equivalently classified field L dwarfs, and furthermore shows no evidence of warm circumstellar material, although these data cannot rule out the presence of a cooler ($\lesssim 300$ K) disk or companion. No warmer companions were resolved in laser guide star adaptive optics observations reported in Bardalez Gagliuffi et al. (2015) to a limit of $\Delta H = 3$ at $0''.2$ (19 AU).

Table 3
Summary of Properties of WISE J0528+0901

Parameter	Value	Reference
α (J2000) ^a	05 ^h 28 ^m 57 ^s .68	1
δ (J2000) ^a	+09°01′04″.4	1
NIR Spectral Type	L1 VLG	2
2MASS J	16.26±0.11	1
2MASS H	15.44±0.12	1
2MASS K_s	14.97±0.11	1
WISE $W1$	14.21±0.03	3
WISE $W2$	13.64±0.04	3
$\mu_\alpha \cos(\delta)$ (mas yr ⁻¹)	-11±10	2
μ_δ (mas yr ⁻¹)	-39±12	2
d (pc) ^b	93±5	2,4
RV (km s ⁻¹)	18±4	2
U (km s ⁻¹) ^b	-11±4	2
V (km s ⁻¹) ^b	-15±5	2
W (km s ⁻¹) ^b	-17±5	2
T_{eff} (K)	1880 ⁺¹⁵⁰ ₋₇₀	2
$\log g$ (cm s ⁻²)	3.8 ^{+0.2} _{-0.2}	2
Age (Myr) ^b	24 ⁺⁴ ₋₃	5
Mass (M_J) ^b	14 ⁺³ ₋₃	2,6

References. — (1) 2MASS (Skrutskie et al. 2006); (2) This work; (3) WISE (Wright et al. 2010); (4) HIPPARCOS (van Leeuwen 2007); (5) Bell et al. (2015); (6) Baraffe et al. (2003).

^a Julian Date Epoch 2451569.7 (2000.07).

^b Assuming membership in the 32 Orionis group.

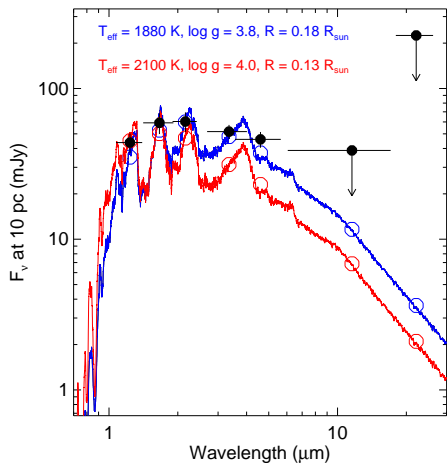


Figure 6. Absolute 2MASS and WISE photometric fluxes for WISE J0528+0901 (black points) assuming a distance of 93±5 pc. The two longest wavelength points are upper limits based on WISE non-detections. These measured fluxes are compared to two BT-Settl spectral models: one with parameters inferred from the L1 VLG classification of the source ($T_{\text{eff}} = 2100$ K, $\log g = 4.0$; red lines and circles), and one with the median parameters from spectral model fitting ($T_{\text{eff}} = 1880$ K, $\log g = 3.8$; blue lines and circles). All models are scaled to agree with absolute 2MASS photometry, and the corresponding radii for those scale factors are listed.

A more detailed analysis of the broad-band spectral properties of WISE J0528+0901, including optical spectroscopy, is needed to assess whether other aspects of this source, such as magnetic emission, are remarkable. WISE J0528+0901 joins a growing list of young,

very low-mass brown dwarfs and planetary-mass objects whose ages, distances, kinematics and compositions (assuming a common initial reservoir of gas and dust) are in common with their more massive siblings. As demonstrated here, these systems provide important validation tests for atmospheric and evolutionary models, while also statistically probing the origins of brown dwarfs in our Galaxy.

The authors thank Jorge Araya at Magellan Observatory for his assistance with the observations, and Richard Faherty for providing a facility to complete this work. We also thank our referee, Derek Homeier, for his prompt and helpful review. The material presented here is based in part on work supported by the National Aeronautics and Space Administration under Grant No. NNX15AI75G, and funding from the McNair Scholars Program. EEM acknowledges support from NSF grant AST-1313029. This research has made use of the SIMBAD database, operated at CDS, Strasbourg, France; NASA’s Astrophysics Data System Bibliographic Services; the M, L, T, and Y dwarf compendium housed at DwarfArchives.org; and the SpeX Prism Libraries housed at <http://www.browndwarfs.org/spexprism>. The authors recognize and acknowledge the very significant cultural role and reverence that the summit of Mauna Kea has always had within the indigenous Hawaiian community. We are most fortunate and grateful to have the opportunity to conduct observations from this mountain.

Facilities: Magellan (FIRE), IRTF (SpeX)

REFERENCES

- Adams, F. C., & Myers, P. C. 2001, *ApJ*, 553, 744
- Aganze, C., Burgasser, A. J., Faherty, J. K., et al. 2015, *ArXiv e-prints*, arXiv:1512.08659
- Allard, F., Homeier, D., & Freytag, B. 2012, *Philosophical Transactions of the Royal Society A*, 370, 2765
- Allers, K. N., & Liu, M. C. 2013, *ApJ*, 772, 79
- Allers, K. N., Jaffe, D. T., Luhman, K. L., et al. 2007, *ApJ*, 657, 511
- Artigau, É., Gagné, J., Faherty, J., et al. 2015, *ApJ*, 806, 254
- Baraffe, I., Chabrier, G., Barman, T. S., Allard, F., & Hauschildt, P. H. 2003, *A&A*, 402, 701
- Bardalez Gagliuffi, D. C., Gelino, C. R., & Burgasser, A. J. 2015, *AJ*, 150, 163
- Bardalez Gagliuffi, D. C., Burgasser, A. J., Gelino, C. R., et al. 2014, *ApJ*, 794, 143
- Barman, T. S., Macintosh, B., Konopacky, Q. M., & Marois, C. 2011, *ApJL*, 735, L39
- Bell, C. P. M., Mamajek, E. E., & Naylor, T. 2015, *MNRAS*, 454, 593
- Blackman, R. B., & Tukey, J. W. 1958, *Bell System Technical Journal*, 37, 185
- Bochanski, J. J., Hennawi, J. F., Simcoe, R. A., et al. 2009, *PASP*, 121, 1409
- Bouy, H., & Alves, J. 2015, *A&A*, 584, A26
- Bressert, E., Bastian, N., Gutermuth, R., et al. 2010, *MNRAS*, 409, L54
- Burgasser, A. J. 2014, *Proceedings of the 2013 International Workshop on Spectral Stellar Libraries*, arXiv:1406.4887
- Burgasser, A. J.,Looper, D. L., Kirkpatrick, J. D., Cruz, K. L., & Swift, B. J. 2008, *ApJ*, 674, 451
- Burrows, A., Hubbard, W. B., Lunine, J. I., & Liebert, J. 2001, *Reviews of Modern Physics*, 73, 719
- Cruz, K. L., Kirkpatrick, J. D., & Burgasser, A. J. 2009, *AJ*, 137, 3345
- Cushing, M. C., Vacca, W. D., & Rayner, J. T. 2004, *PASP*, 116, 362

- Cushing, M. C., Marley, M. S., Saumon, D., et al. 2008, *ApJ*, 678, 1372
- Cutri, R. M., Skrutskie, M. F., van Dyk, S., et al. 2003, *VizieR Online Data Catalog*, 2246, 0
- Delorme, P., Gagné, J., Girard, J. H., et al. 2013, *A&A*, 553, L5
- Dupuy, T. J., & Liu, M. C. 2012, *ApJS*, 201, 19
- Faherty, J. K., Rice, E. L., Cruz, K. L., Mamajek, E. E., & Núñez, A. 2013, *AJ*, 145, 2
- Faherty, J. K., Burgasser, A. J., Walter, F. M., et al. 2012, *ApJ*, 752, 56
- Filippazzo, J. C., Rice, E. L., Faherty, J., et al. 2015, *ApJ*, 810, 158
- Foreman-Mackey, D., Price-Whelan, A., Ryan, G., et al. 2014, *triangle.py* v0.1.1, doi:10.5281/zenodo.11020
- Gagné, J., Lafrenière, D., Doyon, R., Malo, L., & Artigau, É. 2014, *ApJ*, 783, 121
- Gagné, J., Lambrides, E., Faherty, J. K., & Simcoe, R. A. 2015a, *Firehose* v2.0, doi:10.5281/zenodo.18775
- Gagné, J., Faherty, J. K., Cruz, K. L., et al. 2015b, *ApJS*, 219, 33
- Gauza, B., Béjar, V. J. S., Pérez-Garrido, A., et al. 2015, *ApJ*, 804, 96
- Genzel, R., & Stutzki, J. 1989, *ARA&A*, 27, 41
- Gizis, J. E. 2002, *ApJ*, 575, 484
- Gizis, J. E., Allers, K. N., Liu, M. C., et al. 2015, *ApJ*, 799, 203
- Gorlova, N. I., Meyer, M. R., Rieke, G. H., & Liebert, J. 2003, *ApJ*, 593, 1074
- Hastings, W. K. 1970, *Biometrika*, 57, 97
- Hayashi, C., & Nakano, T. 1963, *Progress of Theoretical Physics*, 30, 460
- Jayawardhana, R., Mohanty, S., & Basri, G. 2002, *ApJL*, 578, L141
- Kharchenko, N. V., Piskunov, A. E., Schilbach, E., Röser, S., & Scholz, R.-D. 2013, *A&A*, 558, A53
- Kharchenko, N. V., Scholz, R.-D., Piskunov, A. E., Röser, S., & Schilbach, E. 2007, *Astronomische Nachrichten*, 328, 889
- Kirkpatrick, J. D., Cruz, K. L., Barman, T. S., et al. 2008, *ApJ*, 689, 1295
- Kirkpatrick, J. D., Looper, D. L., Burgasser, A. J., et al. 2010, *ApJS*, 190, 100
- Koenig, X. P., & Leisawitz, D. T. 2014, *ApJ*, 791, 131
- Kumar, S. S. 1962, *AJ*, 67, 579
- . 1963, *ApJ*, 137, 1121
- Lada, C. J., & Lada, E. A. 2003, *ARA&A*, 41, 57
- Lafrenière, D., Jayawardhana, R., & van Kerkwijk, M. H. 2010, *ApJ*, 719, 497
- Looper, D. L., Bochanski, J. J., Burgasser, A. J., et al. 2010a, *AJ*, 140, 1486
- Looper, D. L., Kirkpatrick, J. D., Cutri, R. M., et al. 2008, *ApJ*, 686, 528
- Looper, D. L., Mohanty, S., Bochanski, J. J., et al. 2010b, *ApJ*, 714, 45
- López-Santiago, J., Montes, D., Crespo-Chacón, I., & Fernández-Figueroa, M. J. 2006, *ApJ*, 643, 1160
- Lucas, P. W., Roche, P. F., Allard, F., & Hauschildt, P. H. 2001, *MNRAS*, 326, 695
- Luhman, K. L., D'Alessio, P., Calvet, N., et al. 2005, *ApJL*, 620, L51
- Mamajek, E. E. 2007, in *IAU Symposium*, Vol. 237, IAU Symposium, ed. B. G. Elmegreen & J. Palous, 442–442
- Mamajek, E. E., & Bell, C. P. M. 2014, *MNRAS*, 445, 2169
- Marocco, F., Andrei, A. H., Smart, R. L., et al. 2013, *AJ*, 146, 161
- Marois, C., Macintosh, B., Barman, T., et al. 2008, *Science*, 322, 1348
- McLean, I. S., McGovern, M. R., Burgasser, A. J., et al. 2003, *ApJ*, 596, 561
- Metropolis, N., Rosenbluth, A. W., Rosenbluth, M. N., Teller, A. H., & Teller, E. 1953, *J. Chem. Phys.*, 21, 1087
- Ralchenko, Y., Kramida, A., Reader, J., & NIST ASD Team. 2011, *NIST Atomic Spectra Database* (version 4.1)
- Reid, I. N., Burgasser, A. J., Cruz, K. L., Kirkpatrick, J. D., & Gizis, J. E. 2001, *AJ*, 121, 1710
- Rice, E. L., Faherty, J. K., & Cruz, K. L. 2010, *ApJL*, 715, L165
- Saumon, D., & Marley, M. S. 2008, *ApJ*, 689, 1327
- Schlieder, J. E., Lépine, S., & Simon, M. 2010, *AJ*, 140, 119
- Schneider, A., Song, I., Melis, C., Zuckerman, B., & Bessell, M. 2012, *ApJ*, 757, 163
- Shvonski, A. J., Mamajek, E. E., Meyer, M. R., & Kim, J. S. 2010, in *Bulletin of the American Astronomical Society*, Vol. 42, American Astronomical Society Meeting Abstracts 215, 428.22
- Simcoe, R. A., Burgasser, A. J., Schechter, P. L., et al. 2013, *PASP*, 125, 270
- Skrutskie, M. F., Cutri, R. M., Stiening, R., et al. 2006, *AJ*, 131, 1163
- Spiegel, D. S., Burrows, A., & Milsom, J. A. 2011, *ApJ*, 727, 57
- Stephens, D. C., Leggett, S. K., Cushing, M. C., et al. 2009, *ApJ*, 702, 154
- Thompson, M. A., Kirkpatrick, J. D., Mace, G. N., et al. 2013, *PASP*, 125, 809
- Torres, C. A. O., Quast, G. R., Melo, C. H. F., & Sterzik, M. F. 2008, *Young Nearby Loose Associations*, ed. Reipurth, B., 757
- Vacca, W. D., Cushing, M. C., & Rayner, J. T. 2003, *PASP*, 115, 389
- van Leeuwen, F. 2007, *A&A*, 474, 653
- Wright, E. L., Eisenhardt, P. R. M., Mainzer, A. K., et al. 2010, *AJ*, 140, 1868
- Zuckerman, B., Rhee, J. H., Song, I., & Bessell, M. S. 2011, *ApJ*, 732, 61
- Zuckerman, B., & Song, I. 2004, *ARA&A*, 42, 685